THE JOURNAL OF BIOLOGICAL CHEMISTRY VOL. 290, NO. 1, pp. 65–75, January 2, 2015

HdeB Functions as an Acid-protective Chaperone in Bacteria*

Received for publication, September 19, 2014, and in revised form, November 11, 2014 Published, JBC Papers in Press, November 12, 2014, DOI 10.1074/jbc.M114.612986

Jan-Ulrik Dahl[‡], Philipp Koldewey[‡§], Loïc Salmon[‡§], Scott Horowitz[‡§], James C. A. Bardwell[‡§1], and Ursula Jakob[‡§2]

From the [‡]Department of Molecular, Cellular, and Developmental Biology and the [§]Howard Hughes Medical Institute, University of Michigan, Ann Arbor, Michigan 48109-1048

Background: Periplasmic chaperones HdeA and HdeB are involved in the acid stress response in *Escherichia coli*.
Results: HdeB requires its folded and dimeric state to protect *E. coli* from protein aggregation at pH 4.
Conclusion: HdeA and HdeB use different mechanisms to prevent periplasmic protein aggregation, allowing them to function over a broad pH range.
Significance: This study furthers the understanding of how enteric bacteria counteract acid stress.

Enteric bacteria such as *Escherichia coli* utilize various acid response systems to counteract the acidic environment of the mammalian stomach. To protect their periplasmic proteome against rapid acid-mediated damage, bacteria contain the acid-activated periplasmic chaperones HdeA and HdeB. Activation of HdeA at pH 2 was shown to correlate with its acid-induced dissociation into partially unfolded monomers. In contrast, HdeB, which has high structural similarities to HdeA, shows negligible chaperone activity at pH 2 and only modest chaperone activity at pH 3. These results raised intriguing questions concerning the physiological role of HdeB in bacteria, its activation mechanism, and the structural requirements for its function as a molecular chaperone. In this study, we conducted structural and biochemical studies that revealed that HdeB indeed works as an effective molecular chaperone. However, in contrast to HdeA, whose chaperone function is optimal at pH 2, the chaperone function of HdeB is optimal at pH 4, at which HdeB is still fully dimeric and largely folded. NMR, analytical ultracentrifugation, and fluorescence studies suggest that the highly dynamic nature of HdeB at pH 4 alleviates the need for monomerization and partial unfolding. Once activated, HdeB binds various unfolding client proteins, prevents their aggregation, and supports their refolding upon subsequent neutralization. Overexpression of HdeA promotes bacterial survival at pH 2 and 3, whereas overexpression of HdeB positively affects bacterial growth at pH 4. These studies demonstrate how two structurally homologous proteins with seemingly identical *in vivo* functions have evolved to provide bacteria with the means for surviving a range of acidic protein-unfolding conditions.

Bacteria are exposed to a variety of global environmental stresses, including increased temperature, UV irradiation, and osmotic or pH stresses (1). A prominent example for low pH stress conditions is found in the acidic environment of the mammalian stomach, where pH ranges between 1 and 3 (2) but can increase during fasting periods to pH 4 (3). Acid secretion into the stomach not only plays an important role in the digestion of food, but also serves as an effective barrier against food-borne microbial pathogens (2). However, certain gastrointestinal bacteria such as *Escherichia coli* are able to survive at pH 2.0–2.5 for at least 2 h (4). To survive the acidic environment of the mammalian stomach, these bacteria have evolved strategies that help to cope with the acidification of their intracellular environment and alleviate acid-induced damage.

Transcriptional stress responses are typically highly effective in dealing with stress-related cell damage. However, the delay between the time the stress is initially sensed and the moment defense and repair proteins are functional is problematic when organisms experience fast-acting stressors, such as low pH. Therefore, it is not surprising that cells have developed enzymatic and post-translational mechanisms that allow a more rapid response to these stress conditions (5). Many enteric bacteria employ cytoplasmic amino acid decarboxylases that decarboxylate glutamate, arginine, or lysine in an effort to neutralize excess intra- and extracellular protons (4, 6). In addition, many bacteria are capable of reversing their cytoplasmic membrane potential, thereby reducing proton influx into the cytoplasm and maintaining a more tolerable pH of 4.5 in the cytoplasm (7). However, in contrast to the cytoplasm, which is shielded by the semipermeable plasma membrane, the bacterial periplasm equilibrates almost instantaneously with the environmental pH because the porous outer membrane allows the relatively free diffusion of small (<600 Da) molecules (8). The excess protons can then interact with amino acid residues within polypeptide chains, leading to protein unfolding and aggregation. In turn, this affects the maintenance of biological processes, damages cellular structures, and causes cell death (2, 9). Periplasmic proteins and proteins of the inner membrane are therefore particularly vulnerable to acid stress conditions.

To protect their periplasmic proteome against acid stress, enteric bacterial pathogens contain the small periplasmic chaperones HdeA and HdeB, which use acid stress as a trigger to specifically activate their chaperone function (10, 11). The two genes coding for HdeA and HdeB are part of a larger *hdeA-hdeB* acid stress operon and are induced upon exposure of cells to low pH (12). Their deletion is reported to negatively affect the growth and survival of several enteric bacteria under low pH

* This work was supported, in whole or in part, by National Institutes of Health Grant R01 GM102829 (to J. C. A. B. and U. J.). This work was also supported by the Howard Hughes Medical Institute (to J. C. A. B.).
[1] To whom correspondence may be addressed. Tel.: 734-764-8028; Fax: 734-647-0884; E-mail: jbardwel@umich.edu.
[2] To whom correspondence may be addressed. Tel.: 734-615-1286; Fax: 734-647-0884; E-mail: ujakob@umich.edu.

conditions (10, 11, 13, 14). HdeA and HdeB share 13% sequence identity at the amino acid level, and their structures can be aligned with root mean square deviation of 1.75 Å (15).

HdeA is a well characterized chaperone that protects bacteria against low pH stress. At neutral pH, HdeA is present in its homodimeric chaperone-inactive form. Activation of HdeA occurs within seconds of the pH shift and is triggered by an abrupt drop in pH to <3. Protonation of select negatively charged residues appears to contribute to the dissociation of HdeA dimers into chaperone-active monomers concomitant with the partial unfolding of HdeA (16–18), putting HdeA into the class of conditionally disordered chaperones (19, 20). Upon pH neutralization, HdeA is capable of facilitating the refolding of its client proteins in an ATP-independent matter while returning into its dimeric chaperone-inactive conformation. A "slow-release mechanism" enables HdeA to keep the concentration of aggregation-prone substrate species at very low levels, hence facilitating client refolding (21).

Similar to HdeA, the structurally related HdeB also monomerizes and partially unfolds at pH <3 (10), yet in contrast to HdeA, HdeB displays no significant *in vitro* chaperone activity at pH 2 and has only modest activity when using a periplasmic extract as a substrate at pH 3 (10). The presence of HdeB does, however, promote solubilization of protein aggregates formed at pH 2 (22), implying at least some chaperone function for HdeB at low pH. Given the lack of chaperone activity of HdeB at low pH despite its high structural similarity to HdeA, we wondered about the mechanism of HdeB activation, the structural requirements for HdeB chaperone function, and the physiological role that HdeB plays in bacteria.

Here, we show that the optimal pH of HdeB is 4. Once activated as a chaperone, HdeB binds unfolded client proteins, prevents their aggregation, and facilitates their refolding upon neutralization. In contrast to HdeA, which is active when monomeric and partially unfolded, HdeB remains dimeric and apparently fully folded at pH 4. However, HdeB displays dynamic properties between pH 4 and 7, which apparently allow the chaperone to recognize and bind unfolding proteins at higher pH compared with HdeA. We present a model in which two structurally highly related proteins utilize distinct activation mechanisms that enable them to protect bacteria from the protein-unfolding effects of varying degrees of acid stress conditions.

EXPERIMENTAL PROCEDURES

Bacterial Strains, Plasmids, Media, and Growth Conditions—All strains and plasmids used in this study are listed in Table 1. For *in vivo* survival studies, *hdeA*, *hdeB*, or both *hdeA* and *hdeB* together were amplified from *E. coli* MG1655 using appropriate primers and cloned into the EcoRI and BamHI sites of plasmid pBAD18 to yield plasmids pJUD1, pJUD3, and pJUD5, respectively. Bacterial cultures were grown in LB medium supplemented with either 200 μg/ml ampicillin or 25 μg/ml kanamycin.

Protein Purification—HdeB was expressed from NEB10β cells harboring plasmid pTrc-*hdeB* (see Table 1) and purified following a published protocol (17). HdeB used in the NMR experiments was expressed in M9 medium supplemented with [^{15}N]ammonium chloride (Cambridge Isotope Laboratories, Andover, MA) as sole nitrogen source. Purified and concentrated HdeB was stored in buffer A (50 mM potassium phosphate and 50 mM NaCl (pH 7.5)) and flash-frozen in liquid nitrogen. ^{15}N-Labeled HdeB was stored in citrate buffer (pH 5) supplemented with NMR pH indicators (15 mM sodium citrate, 100 mM NaCl, 0.1 mM EDTA, 4 mM dichloroacetic acid, 0.5 mM dimethylsilapentanesulfonate, 6 mM imidazole, 2 mM piperazine, and 4 mM sodium fluoride). HdeA was expressed and purified as described previously (17).

Chaperone Activity Assays—The influence of purified HdeA and HdeB on the aggregation of guanidine hydrochloride (GdnHCl)[3]-denatured or thermally unfolding malate dehydrogenase (MDH) at different pH values was monitored as described (17, 21, 23). In brief, 150 μM MDH from porcine heart mitochondria (Roche Applied Science) was incubated overnight in 5.4 M GdnHCl, 50 mM potassium phosphate, and 50 mM NaCl (pH 7.5) at room temperature. Guanidine-denatured MDH was then diluted to a final concentration of 2 μM into buffer B (150 mM potassium phosphate, 150 mM NaCl, and 150 mM $(NH_4)_2SO_4$) at the indicated pH that was pre-equilibrated at 25 °C in the presence and absence of various concentrations of HdeB and HdeA, respectively. All listed concentrations of HdeA and HdeB refer to the monomer concentration. After 20 min of incubation, the pH was rapidly raised to 7 by the addition of 0.16–0.34 volume of 2 M K_2HPO_4. Thermal aggregation of MDH was monitored at 43 °C. MDH in buffer A was diluted to a final concentration of 0.5 μM into prewarmed buffer C (150 mM potassium phosphate and 150 mM NaCl) at the indicated pH in the presence and absence of 12.5 μM HdeB. After 20 min of incubation, the pH was raised to 7 by the addition of 0.16–0.34 volume of 2 M unbuffered K_2HPO_4. Thermal aggregation of rabbit muscle lactate dehydrogenase (LDH; Roche Applied Science) was monitored by light scattering at 41 °C. LDH in 40 mM HEPES and 50 mM NaCl (pH 7.5) was diluted to a final concentration of 1 μM into prewarmed buffer C at the indicated pH in the presence and absence of various concentrations of HdeB. After 5 min of incubation, the pH was raised to 7 by the addition of 0.16–0.34 volume of 2 M K_2HPO_4. Changes in absorbance due to the light scattering of protein aggregates were monitored at $\lambda_{ex/em}$ = 350 nm using either a Cary Eclipse fluorescence spectrophotometer (Agilent Technologies, Santa Clara, CA) or an F-4500 fluorescence spectrophotometer (Hitachi, Tokyo, Japan) equipped with temperature-controlled sample holders. HdeA and HdeB activities were normalized to the light-scattering signal of MDH/LDH in the absence of chaperones at each indicated pH.

MDH Unfolding, Refolding, and Activity Assay—The influence of HdeB on the refolding of acid-denatured MDH was analyzed according to Tapley *et al.* (21). In brief, 1 μM MDH was incubated in buffer C at the indicated pH for 1 h at 37 °C in the absence or presence of 25 μM HdeA or HdeB, followed by a 10-min temperature equilibration at 20 °C. Subsequently, the samples were neutralized to pH 7 by the addition of 0.5 M

[3] The abbreviations used are: GdnHCl, guanidine hydrochloride; MDH, malate dehydrogenase; LDH, lactate dehydrogenase; bis-ANS, 4,4′-dianilino-1,1′-binaphthyl-5,5′-disulfonic acid.

TABLE 1
Strains and plasmids used in this study
Sm^R, streptomycin resistance; Km^R, kanamycin resistance; Amp^R, ampicillin resistance.

	Marker	Relevant genotype	Source
Strain			
BL21(DE3)		F^- *ompT gal dcm lon hsdSB* (*rB*$^-$ *mB*$^-$)λ (DE3 (*lacI lacUV5-T7 gene 1 ind1 sam7 nin5*))	Novagen
NEB10β		*Δ(ara-leu) 7697 araD139 fhuA ΔlacX74 galK16 galE15 e14- ϕ80dlacZΔM15 recA1 relA1 endA1 nupG rpsL* (Sm^R) *rph spoT1 Δ(mrr-hsdRMS-mcrBC)*	New England Biolabs
BB7224	Sm^R Km^R	F^- λ$^-$, e14$^-$, $(araD139)_{B/r}$ *Δ(argF-lac)169 flhD5301 Δ(fruK-yeiR)725(fruA25) relA1 rpsL150* (Sm^R) *rbsR22 Δ(fimB-fimE) 632* (::IS1) *ptsF25 zhf::TN10*(*TcS*) *suhX401 deoC1 araD*$^+$ *rpoH::km*$^+$	Ref. 35
Plasmid			
pBAD18	Amp^R	Cloning vector with P_{BAD} arabinose-inducible promoter	Ref. 36
pET21b-*hdeA*	Amp^R	HdeA expression vector	Ref. 17
pTrc-*hdeB*	Amp^R	HdeB expression vector	This study
pJUD1	Amp^R	*hdeA*$^+$ cloned into EcoRI/BamHI sites of pBAD18b	This study
pJUD3	Amp^R	*hdeB*$^+$ cloned into EcoRI/BamHI sites of pBAD18b	This study
pJUD5	Amp^R	*hdeAB*$^+$ cloned into EcoRI/BamHI sites of pBAD18b	This study

sodium phosphate (pH 8) to initiate refolding of acid-denatured MDH. After incubation for 2 h at 20 °C, MDH activity was determined (21). Absorbance was monitored using a Cary 100 spectrophotometer (Agilent Technologies) equipped with a Peltier temperature control block set to 20 °C.

Analytical Ultracentrifugation—Sedimentation velocity experiments with HdeB alone or in complex with thermally unfolding LDH were performed using a Beckman ProteomeLab XL-I analytical ultracentrifuge (Beckman Coulter, Indianapolis, IN). HdeB was diluted to a concentration of 2 μM into buffer C at pH 2–7. To allow HdeB-LDH complex formation, 3 μM LDH was incubated in the presence and absence of 30 μM HdeB in buffer C (pH 4 and 7, respectively) for 15 min at 41 °C prior to sedimentation. All experiments were carried out as follows. Samples were loaded into cells containing standard sector-shaped two-channel Epon centerpieces with 1.2-cm path length and equilibrated to 22 °C for at least 1 h prior to sedimentation. All samples were spun at 48,000 rpm in a Beckman An-50 Ti rotor, and sedimentation of the protein was monitored continuously in intensity mode at either 230 nm (see Fig. 1) or 280 nm (see Fig. 3) using the Beckman ProteomeLab XL-I analytical ultracentrifuge. Data analysis was conducted with SEDFIT (version 14.1) (24) using the continuous *c*(*s*) distribution model. The confidence level for the maximal entropy regularization was set to 0.7. Buffer density and viscosity were calculated using SEDNTERP.

Circular Dichroism—CD measurements were performed at 25 °C using a Jasco J-810 spectropolarimeter. Far-UV CD spectra were recorded using 0.2 mg/ml solutions of protein in 40 mM sodium phosphate buffer at indicated pH.

NMR Spectroscopy—NMR samples were prepared at a concentration of 1 mM ^{15}N-labeled HdeB in 15 mM citrate buffer containing 0.1 mM EDTA and 100 mM NaCl. Dimethylsilapentanesulfonate (0.5 mM) was used for chemical shift referencing, and a solution containing 4 mM dichloroacetic acid, 6 mM imidazole, 2 mM piperazine, and 4 mM formate was used as an internal pH indicator to cover the desired pH range (25, 26). The initial pH was adjusted to 6.8 and was decreased progressively to 2.2 by the addition of 4 mM hydrochloric acid. ^{1}H and ^{15}N chemical shifts were monitored using gradient-based sensitivity-enhanced heteronuclear single-quantum coherence signals, and the pH indicator ^{1}H chemical shifts were recorded in single-dimensional experiments using a WATERGATE (water suppression by gradient-tailored excitation) scheme (27). All NMR experiments were performed at 298 K on a 600-MHz Varian spectrometer equipped with a triple-resonance cryoprobe with pulse-field gradients. All multidimensional spectra were processed using NMRPipe (28) and analyzed using SPARKY3 (29).

Tryptophan Fluorescence and 4,4′-Dianilino-1,1′-binaphthyl-5,5′-disulfonic Acid (Bis-ANS) Binding Studies—HdeB (30 μM) was incubated with 100 μM bis-ANS in buffer C at the indicated pH. After 2 min of incubation at 25 °C, emission spectra were recorded at λ_{ex} = 370 nm. To determine tryptophan fluorescence, 5 μM HdeB was incubated in buffer C at the indicated pH for 5 min at 25 °C. Emission spectra were recorded at λ_{ex} = 370 nm. The Hitachi F-4500 fluorescence spectrophotometer was used.

pH Survival Studies—Plasmids pJUD1 (expressing HdeA), pJUD3 (expressing HdeB), pJUD5 (expressing HdeA and HdeB), and pBAD18 (empty vector control) (Table 1) were transformed into strain BB7224 (Δ*rpoH*) and incubated overnight at 30 °C. Cultures were diluted 1:40 into 25 ml of LB medium supplemented with 200 μg/ml ampicillin and grown in the presence of 0.5% arabinose at 30 °C and 200 rpm to A_{600} = 1.0 to induce HdeA or HdeB protein expression. For the pH shift experiments, cells were diluted to A_{600} = 0.5 with LB medium supplemented with 200 μg/ml ampicillin and 0.5% arabinose and adjusted to the respective pH by the addition of 5 M HCl. After the indicated time points, the cultures were neutralized by the addition of the appropriate volumes of 5 M NaOH. Growth of the neutralized cultures was then monitored in liquid culture for 12 h at 30 °C. Alternatively, cells were diluted in 0.9% NaCl and spot-titered onto LB plates containing 0.5% arabinose. Plates were incubated for 14 h at 30 °C. Each strain was tested at least five independent times.

RESULTS

HdeB Partially Unfolds and Dissociates into Monomers at Low pH—Previous studies suggested that HdeA is activated by pH-induced dissociation and partial unfolding of the monomers (17). The midpoint of HdeA dissociation/unfolding obtained by both bis-ANS fluorescence and FRET measurements was found to be around pH 3.4, consistent with its moderate *in vitro* chaperone activity at pH 3 and high chaperone activity at pH 2 (11, 17, 23). More recent studies using a condi-

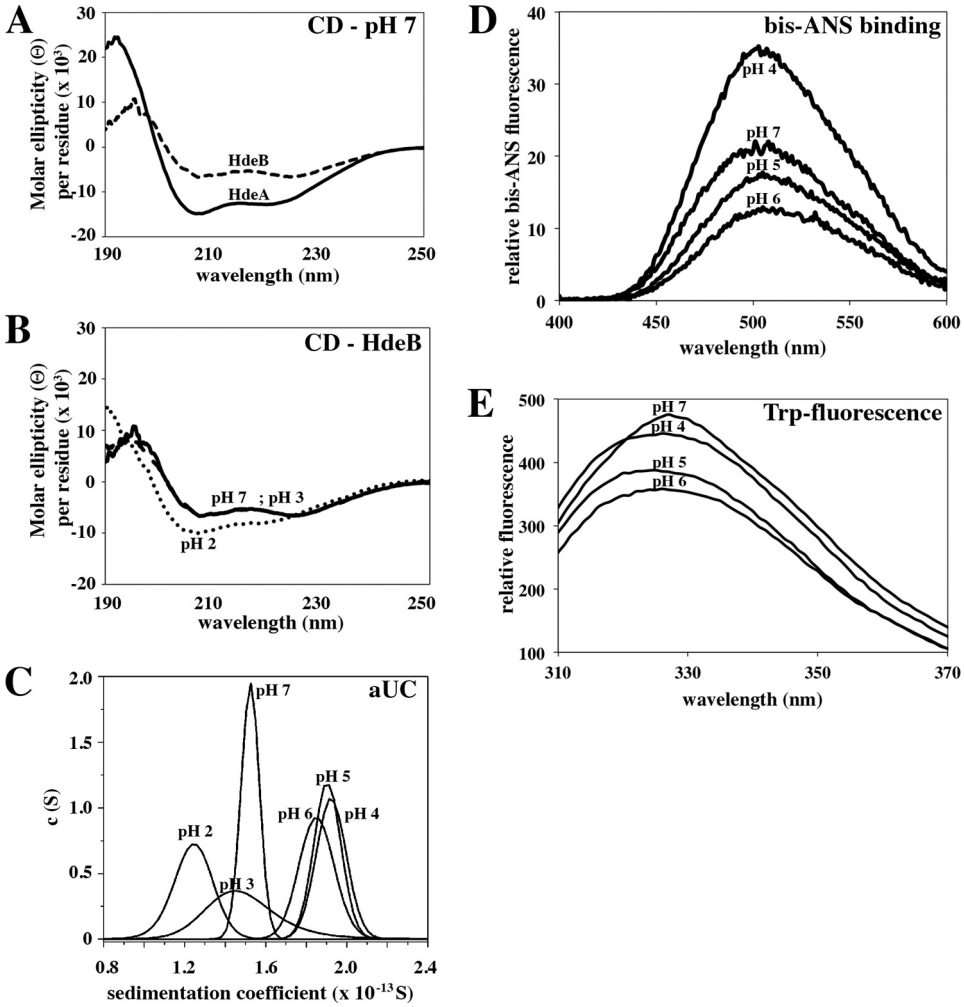

FIGURE 1. **Analysis of the secondary structure of HdeB and its oligomeric state at different pH values.** *A*, far-UV CD spectra of 20.5 μM HdeA (*solid line*) and 22.1 μM HdeB (*dashed line*) in 40 mM phosphate buffer (pH 7). *B*, far-UV CD spectra of 22.1 μM HdeB in 40 mM phosphate buffer at pH 7 (*solid line*), pH 3 (*dashed line*), and pH 2 (*dotted line*). *C*, analytical ultracentrifugation (*aUC*) analysis of 1.8 μM HdeB in buffer C at the indicated pH. Sedimentation velocity data were analyzed with SEDFIT using the continuous *c*(*s*) distribution model. The pH values indicate the respective pH of buffer C at which the oligomeric state of HdeB was analyzed. Bis-ANS fluorescence spectra (*D*) and tryptophan fluorescence spectra (*E*) of HdeB were recorded after incubation at the indicated pH.

tionally active HdeA mutant revealed that the HdeA dimer is stabilized by electrostatic interactions between aspartic and glutamic acid residues on one monomer and positively charged lysine residues on the other monomer (23, 30). Once the pH shifts below the pK_a of the glutamic acid residues, they lose their charge, resulting in the dissociation of the monomers, their partial unfolding, and activation of the chaperone function. In contrast, it has been reported that HdeB has no significant chaperone activity at pH 2 and only modest chaperone activity at pH 3 (10, 22), although fluorescence measurements suggested a HdeA-like midpoint of dissociation/unfolding at pH 3 (10). These results suggested that HdeA and HdeB differ in their mode of functional activation and raised the question about the chaperone-active conformation of HdeB. When we compared the secondary structures of purified HdeA and HdeB at pH 7.0 by far-UV CD spectroscopy, we observed distinct differences (Fig. 1*A*, compare *solid* and *dashed lines*). In solution, HdeB displays significantly lower α-helical content compared with HdeA. Analysis of the secondary structure content using CDSSTR (31) predicted an ~16% lower α-helical content in HdeB compared with HdeA at pH 7. These results suggested that HdeB is significantly less structured and/or more flexible at neutral pH compared with HdeA, a notion that agreed well with the fact that crystallization of HdeB (but not HdeA) was successful only upon reductive methylation (15), a method known to stabilize protein structures (32). Far-UV CD spectra revealed also no major differences in the secondary structure of HdeB upon exposure to pH 4 (data not shown) or pH 3 (Fig. 1*B*, *dashed line*). However, as reported previously (17) and similar to HdeA, partial unfolding of HdeB occurred upon exposure to pH 2 (Fig. 1*B*, *dotted line*). This unfolding of HdeB was found to be fully reversible, and HdeB regained its original structure upon shifting the pH from 2 to 7 (data not shown).

To characterize the structural properties of HdeB in more detail, we next conducted analytical ultracentrifugation experiments at different pH values. We found that HdeB sedimented predominantly in its dimeric form ($s = 1.5 \times 10^{-13}$ S) at pH 7, predominantly in its monomeric form ($s = 1.23 \times 10^{-13}$ S) at pH 2, and as a mixture of dimers and monomers at pH 3 (Fig. 1*C*). These results agreed well with previously conducted fluorescence studies that used the fluorescence quenching of two tryptophan residues in the dimer-dimer interface of HdeB to

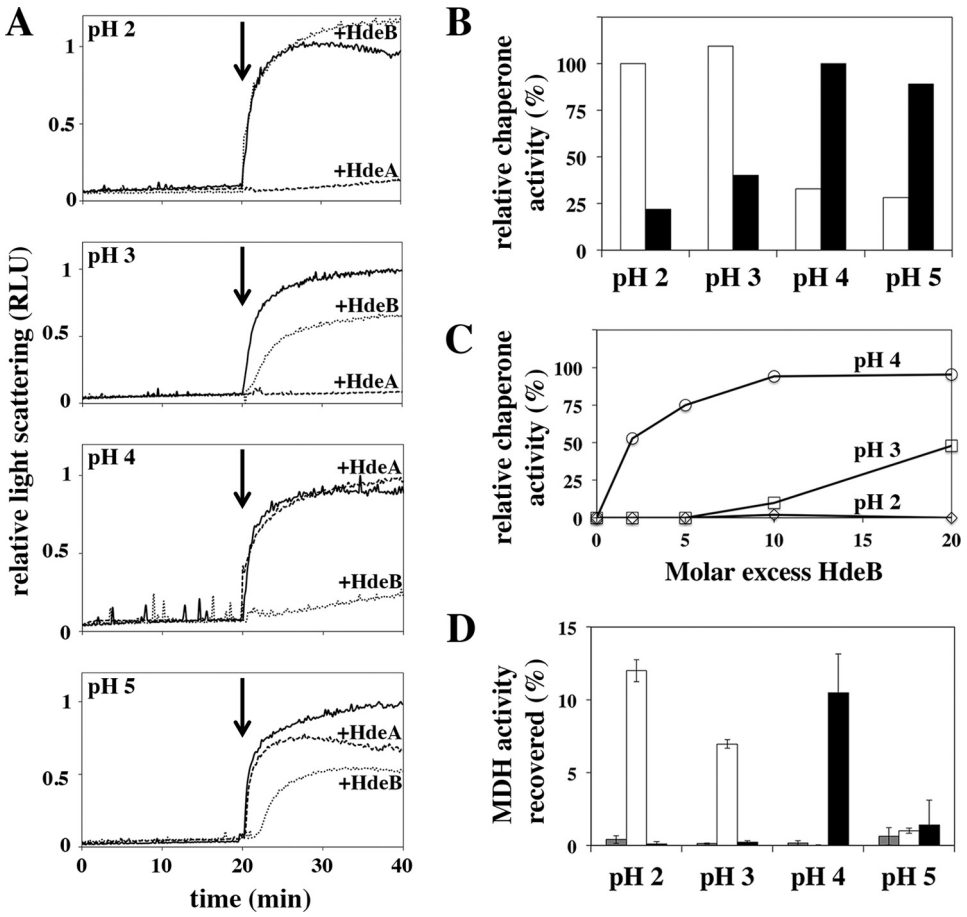

FIGURE 2. **Chaperone activity and refolding ability of HdeA and HdeB at acidic pH.** *A*, GdnHCl-denatured MDH was diluted to a final concentration of 2 μM into buffer B at the indicated pH and incubated for 20 min in the absence (*solid line*) or presence of 20 μM HdeA (*dashed line*) or 50 μM HdeB (*dotted line*). After raising the pH of the samples to 7 by the addition of 0.16 – 0.34 volume of 2 M unbuffered K_2HPO_4 (as indicated by the *arrows*), MDH aggregation was measured by monitoring light scattering at 350 nm. *RLU*, relative light units. *B*, 0.5 μM MDH was incubated in prewarmed buffer C at the indicated pH in the absence or presence of 5 μM HdeA (*black bars*) or 12.5 μM HdeB (*white bars*) for 20 min at 43 °C. MDH aggregation upon neutralization was measured as described for *A*, and the relative chaperone activity was calculated. The activity of HdeA at pH 2 or HdeB at pH 4 was set to 100%. *C*, 1 μM LDH was incubated for 5 min at 41 °C in prewarmed buffer C at the indicated pH in the absence or presence of various concentrations of HdeB. LDH aggregation upon neutralization from pH 2 (◇), pH 3 (□), or pH 4 (○) was measured as described, and the relative chaperone activity was calculated. *D*, 1 μM MDH was incubated in buffer C at the indicated pH for 1 h at 37 °C in the absence or presence of 25 μM HdeA or HdeB. The temperature was then shifted to 20 °C for 10 min before the samples were neutralized to pH 7 by the addition of 0.5 M Na_2HPO_4. Aliquots were taken before and after 2 h of incubation at 20 °C and assayed for MDH activity. MDH activity upon neutralization in the absence of chaperones (*gray bars*) or in the presence of either HdeA (*white bars*) or HdeB (*black bars*) is shown. The mean ± S.D. derived from at least three independent measurements is shown.

monitor its pH-induced dissociation (15). However, to our surprise, we observed substantial changes in the sedimentation behavior of HdeB between pH 7 and 4, where the sedimentation coefficient *s* of HdeB dimers increased as the pH approached 4 (Fig. 1*C*), potentially indicative of a higher HdeB volume due to structural rearrangements at pH 4 compared with pH 7. This result was also consistent with surface hydrophobicity measurements using bis-ANS fluorescence and intrinsic tryptophan fluorescence measurements of HdeB (Fig. 1, *D* and *E*), which showed substantial structural rearrangements in HdeB between pH 4 and 7.

HdeB Shows Maximal in Vitro Chaperone Activity at pH 4—To investigate the influence of pH on the chaperone activity for HdeB, we systematically analyzed the influence of HdeB on the aggregation of several substrate proteins *in vitro* at different pH values. First, we studied the influence of HdeB on the model substrate porcine mitochondrial MDH at different pH values using either chemically denatured (*i.e.* GdnHCl) or thermally denatured MDH. We prepared GdnHCl-denatured MDH and diluted it into reaction buffer with or without chaperones at pH 2–5. Independent of the absence or presence of functional chaperones, MDH remains in an unfolded yet soluble state under these low pH conditions (21). Once neutralized, however, MDH rapidly aggregated unless functional chaperones were present during the low pH incubation period (Fig. 2*A*, *solid lines*). As observed before, GdnHCl-denatured MDH was fully protected by HdeA at pH 2 and 3 (17, 21, 23), and no significant MDH aggregation was observed upon neutralization under these low pH conditions (Fig. 2*A*, *dashed lines*). At higher pH, however, HdeA almost completely failed to protect MDH from aggregation. In contrast, the presence of HdeB did not affect aggregation of MDH upon its neutralization from pH 2, moderately reduced MDH aggregation upon its neutralization from pH 3 or 5, and almost completely suppressed aggregation upon neutralization from pH 4 (Fig. 2*A*, *dotted lines*). These results suggest that HdeB chaperone function has a pH optimum around 4, which is in a significantly higher pH range than reported previously (10, 22) and higher than that of HdeA. Fur-

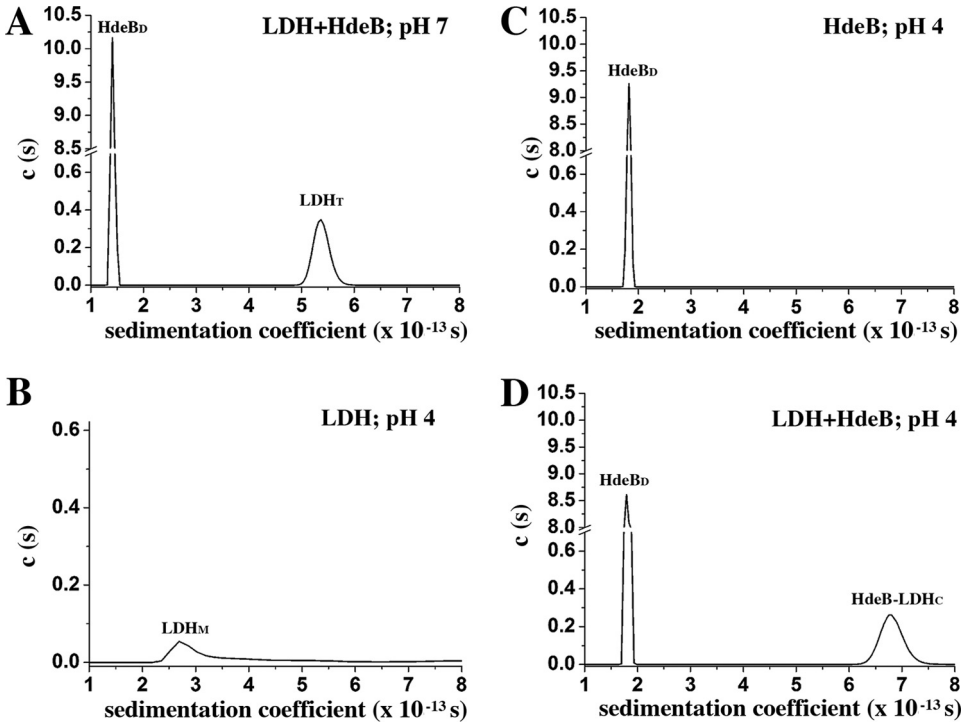

FIGURE 3. **Complex formation of HdeB dimers with unfolded LDH at pH 4 by analytical ultracentrifugation.** LDH (3 μM) was incubated in the presence of a 10-fold molar excess of HdeB in buffer C for 15 min at 41 °C and pH 7 (*A*) or pH 4 (*D*). For comparison, LDH alone (*B*) or HdeB alone (*C*) was incubated for 15 min at 41 °C and pH 4. The results from analytical ultracentrifugation sedimentation velocity analysis are shown. Sedimentation coefficient distribution (*c*(*s*)) was analyzed using SEDFIT. LDH_T, LDH tetramer; LDH_M, LDH monomer; $HdeB_D$, HdeB dimer; $HdeB\text{-}LDH_C$, HdeB-LDH complex.

thermore, HdeB becomes active as a chaperone substantially before monomerization and partial unfolding occur (Fig. 1). To exclude that the folding state of the client protein affects HdeB function, we analyzed the chaperone activity of HdeB at different pH values using thermally denatured MDH as client. For these experiments, native MDH was diluted into 43 °C buffer at the indicated pH with or without HdeA or HdeB present. As before, aggregation of MDH was triggered by neutralizing the reaction buffer at 43 °C. Consistent with our results using chemically denatured MDH, we found that HdeA prevented aggregation of thermally unfolding MDH upon neutralization from pH 2 or 3 (Fig. 2*B*, *white bars*), whereas HdeB reduced MDH aggregation upon its neutralization from pH 4 or 5 (*black bars*). Very similar results were also obtained when we used thermally unfolding LDH, where the presence of a 20-fold excess of HdeB had no effect on the aggregation of LDH at pH 2, whereas a 2-fold molar excess of HdeB significantly reduced aggregation upon LDH dilution at pH 4 (Fig. 2*C*). We concluded from these results that independent of the client proteins or the method of client unfolding, HdeB appears to have its optimal chaperone activity around pH 4 and that this optimum is significantly above the pH range at which monomerization and unfolding occur (pH <4).

HdeB Facilitates Refolding of MDH Optimally at pH 4—HdeA is known to support the refolding of pH 2-unfolded proteins once neutralizing conditions are restored (21). To compare the foldase activity of HdeA and HdeB, we incubated thermally denatured MDH at different pH values in the presence of either chaperone, neutralized the pH to initiate refolding, and determined the activity of MDH after 2 h. As shown in Fig. 2*D*, in the absence of HdeA or HdeB, acid-denatured MDH had a very low propensity for spontaneous refolding, resulting in <1% MDH activity independent of the original pH conditions (Fig. 2*D*, *gray bars*). Consistent with previous reports (21), we found that in the presence of HdeA, substantial reactivation of MDH was achieved upon neutralization from pH 2 or 3, but not upon neutralization from pH 4 and 5 (Fig. 2*D*, *white bars*). In the presence of HdeB, however, significant reactivation of MDH was achieved only upon neutralization from pH 4 (Fig. 2*D*, *black bars*). We concluded from these results that much like HdeA, HdeB is able to protect proteins against pH-induced aggregation and facilitates their reactivation upon neutralization. The major difference between these two proteins lies within their optimal pH at which they fulfill this important task.

HdeB Dimers Form Complexes with Client Proteins at pH 4—Our previous results suggested that in contrast to HdeA, which is chaperone-active when monomeric and partially unfolded, HdeB works in its dimeric conformation. To directly monitor the complex formation between HdeB and client proteins, we used analytical ultracentrifugation analysis. We incubated HdeB and its client protein LDH at either pH 7 or 4 for 15 min at 41 °C, cooled the reaction down, and performed analytical ultracentrifugation experiments at 22 °C. Upon incubation of the two proteins at pH 7, we did not observe any complex formation (Fig. 3*A*). As in the absence of additional proteins, HdeB at 22 °C sedimented predominantly in its dimeric state ($s = 1.45 \times 10^{-13}$ S) (Fig. 3, *A* and *C*), indicating that elevated temperatures do not affect its oligomerization state at pH 7 or 4. LDH was present exclusively as a tetramer, the biologically active state, confirming the observation that LDH was not sub-

TABLE 2
Summary of analytical ultracentrifugation data

	Sample	Oligomeric state	Mass
			kDa
Fig. 3*A*	LDH + HdeB (pH 7)	HdeB dimer	16.4
		LDH tetramer	120
Fig. 3*B*	LDH (pH 4)	Monomer	44.1
Fig. 3*C*	HdeB (pH 4)	Dimer	18.2
Fig. 3*D*	LDH + HdeB (pH 4)	HdeB dimer	18.3
		LDH-HdeB complex	134

stantially unfolded upon incubation at 41 °C ($s = 5.4 \times 10^{-13}$ S) (Fig. 3*A*). After heat treatment of LDH at pH 4, however, 38% of LDH sedimented before the first scan was recorded, likely as large aggregates, whereas the remaining LDH appeared to sediment predominantly as monomers (Fig. 3*B*). When LDH was incubated in the presence of HdeB at pH 4 and 41 °C, no aggregation was observed prior to the sedimentation, consistent with our *in vitro* aggregation measurements. Moreover, we detected a large species, indicated as HdeB-LDH_C ($s = 6.8 \times 10^{-13}$ S, calculated molecular mass of 134 kDa), which differed significantly in sedimentation coefficient from the LDH tetramer (calculated molecular mass of 120 kDa) found at pH 7, the MDH monomer found at pH 4, or HdeB dimers (calculated molecular mass of 18 kDa) found at either pH 7 or 4 (Fig. 3*D* and Table 2). Together with the observation that the HdeB dimer peak significantly decreased in the presence of thermally unfolding MDH at pH 4, we concluded from these results that the 134-kDa species likely represents a complex between HdeB dimers and thermally unfolding MDH tetramers.

HdeA and HdeB Appear to Cooperate in Protecting E. coli against a Variety of Low pH Stress Conditions—Our studies indicated that HdeA and HdeB both bind acid-denatured client proteins and facilitate their reactivation upon neutralization. However, whereas HdeA is active at pH 2–3, HdeB appears to be predominantly chaperone-active at pH 4. We therefore wondered if this largely non-overlapping pH optimum would allow HdeA and HdeB to protect bacteria from the full range of protein-unfolding low pH conditions that bacteria typically encounter in their environment (2, 9). To analyze if this is the case *in vivo*, we conducted survival assays. We utilized the mutant *E. coli* strain BB7224 (Δ*rpoH*), which lacks the σ factor required for the expression of the heat shock response system and is known to be more sensitive to environmental stress conditions than wild-type *E. coli* (33). We increased the levels of periplasmic HdeA, HdeB, or HdeA/HdeB by plasmid-induced overexpression; added defined amounts of HCl to adjust the media pH; incubated the cells for the indicated times; and neutralized the culture by the addition of 5 M NaOH. Subsequently, we monitored growth in liquid culture or survival on plates.

When HdeA, HdeB, or HdeA/HdeB were overexpressed under neutral pH conditions, all strains grew comparably to the control strain, which harbors the empty vector pBAD18 (Fig. 4*A*). However, when cells were incubated at pH 2 for 1 min, only bacteria expressing additional HdeA were able to resume growth after the treatment (Fig. 4*B*, *upper left panel*). Spot titers on plates performed immediately following neutralization revealed a 10–100-fold higher survival rate of acid treatment for strains expressing HdeA either alone or in combination with HdeB (Fig. 4*B*, *upper right panel*). However, elevated amounts of HdeB failed to protect bacteria at this pH. The fact that both proteins contain the N-terminal leader peptide and hence compete for Sec-dependent transport to the periplasm may explain the lower survival rate of strains overexpressing both HdeA and HdeB. Alternatively, higher affinity of the Sec system for HdeB might make it the preferred protein to be transported under these overexpression conditions. Similar results were obtained at pH 3, although at this pH, some protective effect was also observed for strains expressing HdeB alone (Fig. 4*B*, *middle panels*). In contrast to the very fast and highly toxic effects of pH 2 or 3, we observed no significant cell killing when cells were incubated at pH 4. However, cells showed differences in their ability to resume growth after the acid treatment, with strains overexpressing HdeB either alone or in combination with HdeA revealing reproducibly better growth than the strain expressing only HdeA or, even more pronounced, the strain carrying the empty vector control (Fig. 4*B*, *lower panels*). Our *in vivo* survival studies thus support the *in vitro* studies and indicate that HdeA functions at pH 2–3, whereas HdeB adopts its protective role when *E. coli* cells are exposed to less severe acid stress.

HdeB Dimers Are Highly Dynamic between pH 5.6 and 2.8—HdeA has been shown to undergo a dimer-to-monomer transition and partially unfolds at pH ≤3, which correlates well with its activation as a chaperone. In contrast, although structurally very similar to HdeA, HdeB appears to be fully chaperone-active at pH 4 in its predominantly dimeric and folded state and, also in contrast to HdeA, inactivates upon dissociation and unfolding. These results suggested that more subtle structural changes might contribute to the activation of HdeB as chaperone at pH 4. Indeed, our ultracentrifugation studies suggested conformational alterations of HdeB at pH 4–7 (Fig. 1*C*). We therefore decided to focus on this pH range and used NMR spectroscopy to investigate the structural changes of HdeB in more detail. On average in this range of pH, we observed ~60 of the expected 73 peaks of HdeB. The remaining resonances were apparently broadened beyond detection possibly by a conformational exchange process (Fig. 5). This well dispersed nature of the resonances, which is characteristic for a well folded protein, was observed at all pH values above 3, consistent with our spectroscopic measurements indicating that global unfolding occurred below this pH. In addition, we observed several structural and dynamic changes in HdeB over the studied pH range. For example, by increasing the pH from 5.6 to 6.8 (Fig. 5, *upper panel*), we observed a transition that manifested itself through the complete disappearance of several HdeB resonances, with a very limited number of chemical shift changes, suggesting that a structural change occurs on a relatively slow NMR timescale. At pH 5.6 and 2.8, where HdeB is expected to be mostly dimeric at the tested concentration (1 mM), we observed significant chemical shift changes, affecting most of the observed resonances (Fig. 5, *middle panel*). These results indicate that although HdeB retains its overall fold, significant conformational changes occur on a fast-exchange regime. These structural changes are probably primarily due to protonation of pH-sensitive residues. At lower pH (pH 2.8 and 2.2), we observed a sharp transition upon which most of the signals of HdeB disap-

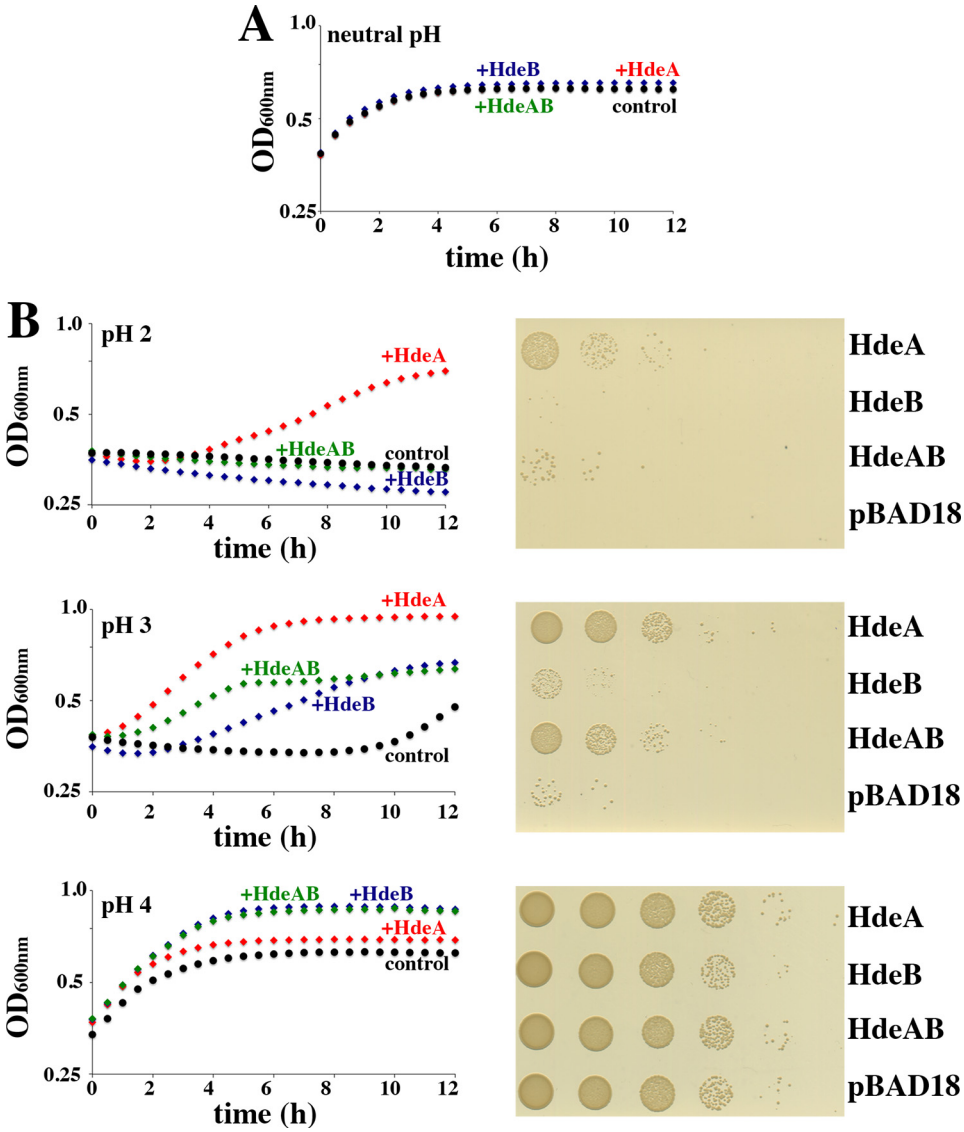

FIGURE 4. **HdeB and HdeA work independently to protect *E. coli* against acidic pH.** HdeA (*red*), HdeB (*blue*), or HdeA and HdeB (*HdeAB*; *green*) were overexpressed in BB7224 (Δ*rpoH*) in the presence of 0.5% arabinose at 30 °C. BB7224 cells harboring the empty vector pBAD18 were used as a control (*black*). *A*, growth of the four strains was monitored at 30 °C. *B*, cells were shifted to the indicated pH by the addition of 5 M HCl and incubated for 1 min at pH 2 (*upper panels*), 2.5 min at pH 3 (*middle panels*), and 30 min at pH 4 (*lower panels*). Subsequently, cultures were neutralized upon the addition of the appropriate volumes of 5 M NaOH. Growth was monitored in liquid medium at 30 °C (*left panels*), or cells were diluted immediately upon neutralization in 0.9% (w/v) NaCl and spot-titered onto LB plates containing 0.5% arabinose (*right panels*). Plates were incubated for 14 h at 30 °C. Each strain was tested at least five independent times.

peared from the spectra (Fig. 5, *lower panel*). This transition likely corresponds to the monomerization of HdeB, causing at least partial unfolding, as suggested by the decrease in the range of observed chemical shifts. Additional experiments, including the assignment of the HdeB spin system, are now necessary to further define the changes in HdeB that contribute to its activation. However, we can conclude from these studies that the conformational properties of HdeB are highly pH-sensitive at a pH range that coincides with its activation as a chaperone. At neutral and very low pH, however, slower conformational transitions appear, potentially defining the limit of HdeB chaperone activity.

DISCUSSION

Many proteins are susceptible to acid-mediated denaturation. The presence of pores in the outer membrane of Gram-negative bacteria thus makes the periplasmic proteome a vulnerable target of acid stress in bacteria (10, 16, 34). To chaperone protein folding under these low pH conditions, enteric bacteria such as *E. coli* encode several stress-specific chaperones, including HdeA, whose acid-induced activation protects proteins against the otherwise lethal protein aggregation. Triggered by a downshift to pH <3, HdeA monomerizes and partially unfolds, allowing it to bind and protect other acid-denatured proteins as long as the pH remains low (16, 17, 21, 23). Upon neutralization, HdeA slowly releases its client proteins. This mechanism keeps the concentration of aggregation-sensitive intermediates low and facilitates protein refolding (21). It has been previously shown that HdeA is only modestly active at pH 3 and inactive at pH 4, raising the question about how *E. coli* cells withstand moderately acidic stress conditions. In this study, we investigated HdeB, a structural homolog of

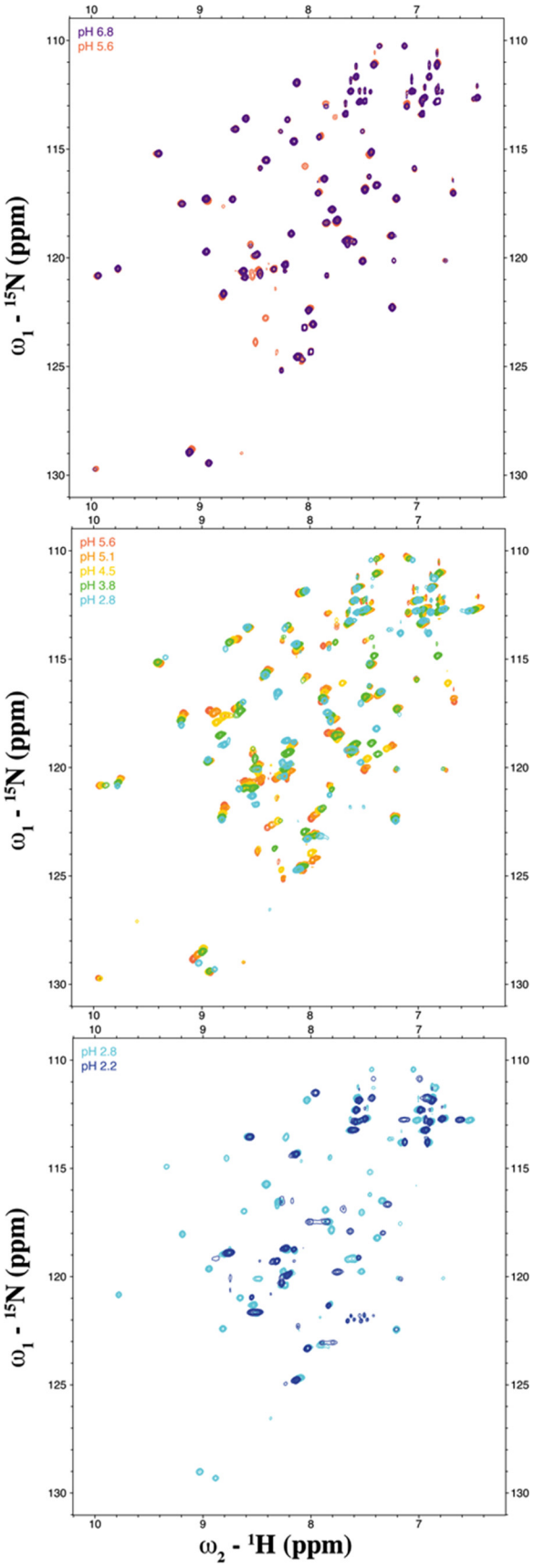

FIGURE 5. **pH-induced conformational changes in HdeB followed by NMR.** Shown are ^{1}H-^{15}N heteronuclear single-quantum coherence signals of HdeB at various pH values: pH 6.8 (*purple*), pH 5.6 (*coral*), pH 5.1 (*orange*), pH 4.5 (*yellow*), pH 3.8 (*green*), pH 2.8 (*cyan*), and pH 2.2 (*blue*).

HdeA, and the second *E. coli* protein suggested to protect periplasmic proteins against acid stress (10, 22). We presented evidence that HdeB is a molecular chaperone that functions at a pH range that is still potentially bactericidal but significantly higher than the pH range in which HdeA is optimally active. *In vitro* chaperone studies using different client proteins established that HdeB exhibits optimal chaperone activity around pH 4–5. Our studies show that similar to HdeA, HdeB is a dimer at neutral pH and dissociates into monomers at pH 2–3, which is accomplished by at least partial unfolding of the monomers. However, unlike for HdeA, which is partially unfolded at its optimal pH of <3, activation of HdeB clearly precedes acid-induced monomerization. These results suggest that the hydrophobic surface of the dimerization interface, which has been the proposed client-binding site in HdeA (17), is unlikely to serve for substrate binding in HdeB. The unifying feature between the two proteins, which share high structural but very limited sequence homology, may be a pH-mediated increase in flexibility that triggers their chaperone activity. In fact, our NMR, fluorescence, and analytical ultracentrifugation studies demonstrated that HdeB is a very dynamic protein and suggested substantial structural rearrangements upon reaching the activating pH of 4. These results suggest that the structural changes that we observed between pH 4 and 7 are sufficient for activation of HdeB chaperone function. It now remains to be tested whether the activation mechanisms of HdeA and HdeB are fundamentally different or whether activation of both proteins involves similar, potentially more local rearrangements, which, in the case of HdeA, coincide with and are masked by the more global unfolding events. Future studies may involve constant pH molecular dynamics calculations based on the crystal structure of HdeB. This approach was successfully used to identify amino acid residues crucial for the acid-induced activation of HdeA (23).

With these findings, we now present a working model illustrating how the acid-activated chaperones HdeA and HdeB assist during acid stress and recovery in *E. coli* (Fig. 6). At neutral pH, both HdeA and HdeB are present as well folded dimers. Upon a shift to pH 2, as usually occurs upon entering the mammalian stomach, HdeA and HdeB rapidly monomerize and partially unfold. Whereas HdeB is reversibly inactivated under these acid-stress conditions, HdeA undergoes structural changes that allow it to tightly interact with unfolding client proteins and inhibit their acid-induced aggregation. Upon transition back to pH 7, as occurs between the stomach and small intestine, proteins can now directly refold upon release from HdeA. A slow transition to neutral pH might cause the inactivation of HdeA and the subsequent release of the substrates at pH >3. At pH 4–5, HdeB may then bind the released substrates to prevent them from aggregation. HdeB might have a more physiologically important role during extended fasting periods, when the pH of the mammalian stomach is increased to pH 4 (3). These conditions are still acidic enough to be denaturing but no longer activate HdeA. Then, HdeB can take over the function of HdeA and promote protein protection. The presence of both HdeA and HdeB therefore appears to enable *E. coli* cells to rapidly respond to a variety of acid stress conditions at a

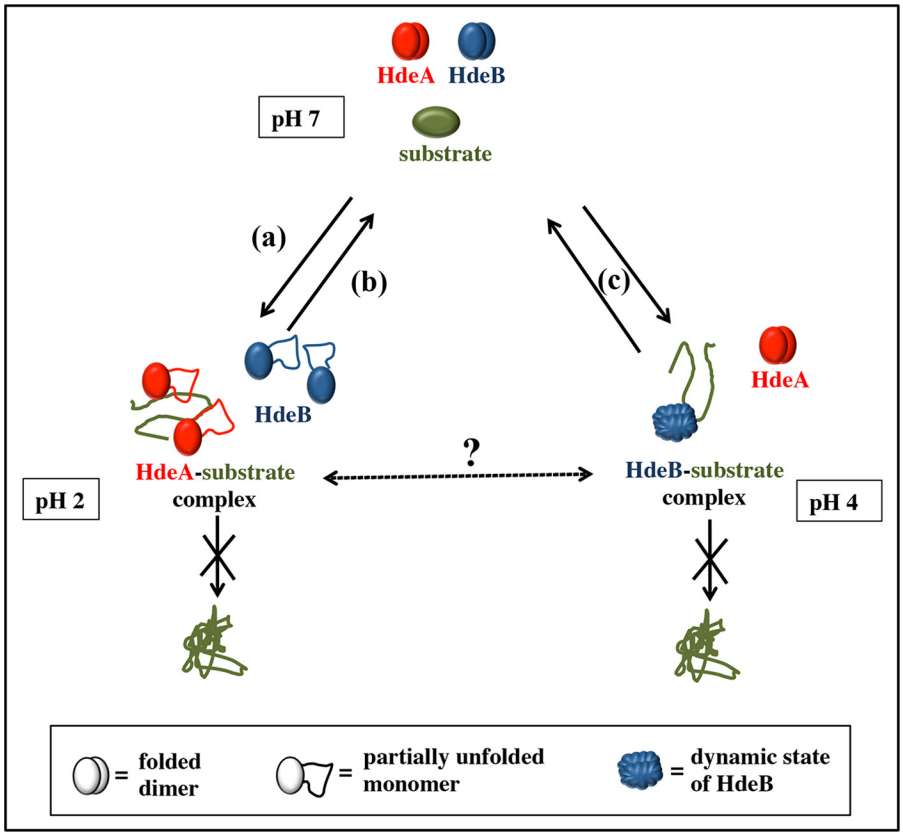

FIGURE 6. **Model for the mechanism of the acid-activated chaperones HdeA and HdeB.** At pH 7, both HdeA (*red*) and HdeB (*blue*) are inactive dimers. Upon a shift to pH 2, as occurs in the mammalian stomach, HdeA and HdeB rapidly monomerize and partially unfold (*arrow a*). Whereas HdeB is inactive in this form, partially unfolded HdeA monomers tightly bind to unfolding client proteins (*green*) and inhibit their acid-induced aggregation. Fast neutralization (*arrow b*) triggers the release of unfolded substrate proteins, which subsequently refold. Upon slow neutralization (pH 4), HdeA and HdeB both refold. Whereas HdeA is inactive in this state, HdeB is now active and could potentially bind the unfolded client proteins until neutral pH conditions are restored. During fasting periods (*arrow c*), the pH of the mammalian stomach is increased to pH 4. Under these conditions, only HdeB is active and protects client proteins from pH 4-mediated protein unfolding and aggregation.

broader pH range, minimizing the irreversible aggregation of acid-unfolded proteins.

Acknowledgments—We thank Dr. Claudia Cremers for helpful advice on chaperone biology and Dr. Linda Foit for critically reading the manuscript. Ken Wan is acknowledged for technical assistance in HdeB purification.

REFERENCES

1. Jakob, U., Kriwacki, R., and Uversky, V. N. (2014) Conditionally and transiently disordered proteins: awakening cryptic disorder to regulate protein function. *Chem. Rev.* **114,** 6779–6805
2. Smith, J. L. (2003) The role of gastric acid in preventing foodborne disease and how bacteria overcome acid conditions. *J. Food Prot.* **66,** 1292–1303
3. Ward, F. W., and Coates, M. E. (1987) Gastrointestinal pH measurement in rats: influence of the microbial flora, diet and fasting. *Lab. Anim.* **21,** 216–222
4. Foster, J. W. (2004) *Escherichia coli* acid resistance: tales of an amateur acidophile. *Nat. Rev. Microbiol.* **2,** 898–907
5. Chuang, S. E., and Blattner, F. R. (1993) Characterization of twenty-six new heat shock genes of *Escherichia coli*. *J. Bacteriol.* **175,** 5242–5252
6. Lin, J., Lee, I. S., Frey, J., Slonczewski, J. L., and Foster, J. W. (1995) Comparative analysis of extreme acid survival in *Salmonella typhimurium*, *Shigella flexneri*, and *Escherichia coli*. *J. Bacteriol.* **177,** 4097–4104
7. Richard, H., and Foster, J. W. (2004) *Escherichia coli* glutamate- and arginine-dependent acid resistance systems increase internal pH and reverse transmembrane potential. *J. Bacteriol.* **186,** 6032–6041
8. Koebnik, R., Locher, K. P., and Van Gelder, P. (2000) Structure and function of bacterial outer membrane proteins: barrels in a nutshell. *Mol. Microbiol.* **37,** 239–253
9. Hong, W., Wu, Y. E., Fu, X., and Chang, Z. (2012) Chaperone-dependent mechanisms for acid resistance in enteric bacteria. *Trends Microbiol.* **20,** 328–335
10. Kern, R., Malki, A., Abdallah, J., Tagourti, J., and Richarme, G. (2007) *Escherichia coli* HdeB is an acid stress chaperone. *J. Bacteriol.* **189,** 603–610
11. Gajiwala, K. S., and Burley, S. K. (2000) HDEA, a periplasmic protein that supports acid resistance in pathogenic enteric bacteria. *J. Mol. Biol.* **295,** 605–612
12. Tucker, D. L., Tucker, N., and Conway, T. (2002) Gene expression profiling of the pH response in *Escherichia coli*. *J. Bacteriol.* **184,** 6551–6558
13. Valderas, M. W., Alcantara, R. B., Baumgartner, J. E., Bellaire, B. H., Robertson, G. T., Ng, W.L., Richardson, J. M., Winkler, M. E., and Roop, R. M., 2nd (2005) Role of HdeA in acid resistance and virulence in *Brucella abortus* 2308. *Vet. Microbiol.* **107,** 307–312
14. Waterman, S. R., and Small, P. L. C. (1996) Identification of sigma S-dependent genes associated with the stationary-phase acid-resistance phenotype of *Shigella flexneri*. *Mol. Microbiol.* **21,** 925–940
15. Wang, W., Rasmussen, T., Harding, A. J., Booth, N. A., Booth, I. R., and Naismith, J. H. (2012) Salt bridges regulate both dimer formation and monomeric flexibility in HdeB and may have a role in periplasmic chaperone function. *J. Mol. Biol.* **415,** 538–546
16. Hong, W., Jiao, W., Hu, J., Zhang, J., Liu, C., Fu, X., Shen, D., Xia, B., and Chang, Z. (2005) Periplasmic protein HdeA exhibits chaperone-like activity exclusively within stomach pH range by transforming into disordered conformation. *J. Biol. Chem.* **280,** 27029–27034

17. Tapley, T. L., Körner, J. L., Barge, M. T., Hupfeld, J., Schauerte, J. A., Gafni, A., Jakob, U., and Bardwell, J. C. A. (2009) Structural plasticity of an acid-activated chaperone allows promiscuous substrate binding. *Proc. Natl. Acad. Sci. U.S.A.* **106,** 5557–5562
18. Zhang, B. W., Brunetti, L., and Brooks, C. L., 3rd (2011) Probing pH-dependent dissociation of HdeA dimers. *J. Am. Chem. Soc.* **133,** 19393–19398
19. Reichmann, D., Xu, Y., Cremers, C. M., Ilbert, M., Mittelman, R., Fitzgerald, M. C., and Jakob, U. (2012) Order out of disorder: working cycle of an intrinsically unfolded chaperone. *Cell* **148,** 947–957
20. Bardwell, J. C. A., and Jakob, U. (2012) Conditional disorder in chaperone action. *Trends Biochem. Sci.* **37,** 517–525
21. Tapley, T. L., Franzmann, T. M., Chakraborty, S., Jakob, U., and Bardwell, J. C. A. (2010) Protein refolding by pH-triggered chaperone binding and release. *Proc. Natl. Acad. Sci. U.S.A.* **107,** 1071–1076
22. Malki, A., Le, H. T., Milles, S., Kern, R., Caldas, T., Abdallah, J., and Richarme, G. (2008) Solubilization of protein aggregates by the acid stress chaperones HdeA and HdeB. *J. Biol. Chem.* **283,** 13679–13687
23. Foit, L., George, J. S., Zhang, B. W., Brooks, C. L., 3rd, and Bardwell, J. C. A. (2013) Chaperone activation by unfolding. *Proc. Natl. Acad. Sci. U.S.A.* **110,** E1254–E1262
24. Schuck, P. (2000) Size-distribution analysis of macromolecules by sedimentation velocity ultracentrifugation and Lamm equation modeling. *Biophys. J.* **78,** 1606–1619
25. Baryshnikova, O. K., Williams, T. C., and Sykes, B. D. (2008) Internal pH indicators for biomolecular NMR. *J. Biomol. NMR* **41,** 5–7
26. Szakács, Z., Hägele, G., and Tyka, R. (2004) $^{1}H/^{31}P$ NMR pH indicator series to eliminate the glass electrode in NMR spectroscopic pK_a determinations. *Anal. Chim. Acta* **522,** 247–258
27. Piotto, M., Saudek, V., and Sklenár, V. (1992) Gradient-tailored excitation for single-quantum NMR spectroscopy of aqueous solutions. *J. Biomol. NMR* **2,** 661–665
28. Delaglio, F., Grzesiek, S., Vuister, G. W., Zhu, G., Pfeifer, J., and Bax, A. (1995) NMRPipe: a multidimensional spectral processing system based on UNIX pipes. *J. Biomol. NMR* **6,** 277–293
29. Goddard, T. D., and Kneller, D. G. (2008) *SPARKY3*, University of California, San Francisco, CA
30. Zhang, M., Lin, S., Song, X., Liu, J., Fu, Y., Ge, X., Fu, X., Chang, Z., and Chen, P. R. (2011) A genetically incorporated crosslinker reveals chaperone cooperation in acid resistance. *Nat. Chem. Biol.* **7,** 671–677
31. Whitmore, L., and Wallace, B. A. (2008) Protein secondary structure analyses from circular dichroism spectroscopy: methods and reference databases. *Biopolymers* **89,** 392–400
32. Fan, Y., and Joachimiak, A. (2010) Enhanced crystal packing due to solvent reorganization through reductive methylation of lysine residues in oxidoreductase from *Streptococcus pneumoniae*. *J. Struct. Funct. Genomics* **11,** 101–111
33. Parker, B. W., Schwessinger, E. A., Jakob, U., and Gray, M. J. (2013) RclR is a reactive chlorine-specific transcription factor in *Escherichia coli*. *J. Biol. Chem.* **288,** 32574–32584
34. Goto, Y., Calciano, L. J., and Fink, A. L. (1990) Acid-induced folding of proteins. *Proc. Natl. Acad. Sci. U.S.A.* **87,** 573–577
35. Tomoyasu, T., Mogk, A., Langen, H., Goloubinoff, P., and Bukau, B. (2001) Genetic dissection of the roles of chaperones and proteases in protein folding and degradation in the *Escherichia coli* cytosol. *Mol. Microbiol.* **40,** 397–413
36. Guzman, L. M., Belin, D., Carson, M. J., and Beckwith, J. (1995) Tight regulation, modulation, and high-level expression by vectors containing the arabinose P_{BAD} promoter. *J. Bacteriol.* **177,** 4121–4130